PNAS
www.pnas.org

Supplementary Information for

A non-canonical role for the binding protein in substrate uptake by the MetNI methionine ATP Binding Cassette (ABC) importer

Phong T. Nguyen, Jeffrey Y. Lai, Allen T. Lee, Jens T. Kaiser, Douglas C. Rees

corresponding author:
Douglas C. Rees
Email: dcrees@caltech.edu

This PDF file includes:

Figs. S1 to S6
Table S1

www.pnas.org/cgi/doi/10.1073/pnas.1811003115

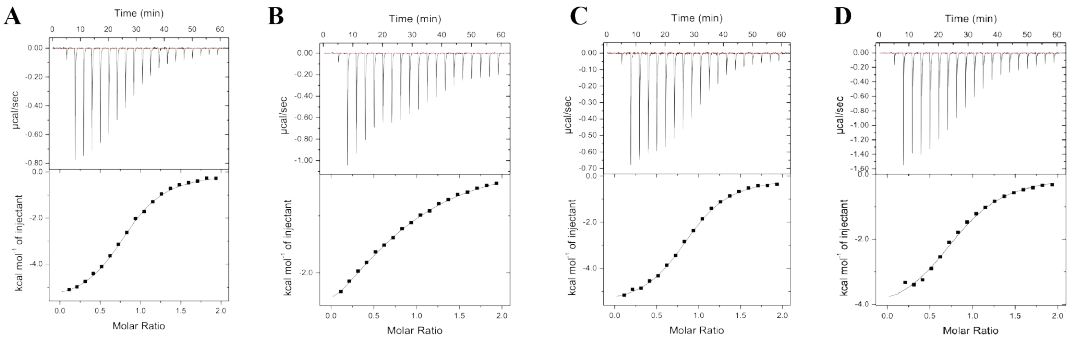

wt MetQ to D-met	NA MetQ to D-met	wt MetQ to D-semet	NA MetQ to D-semet
K_d = 7.5 ± 1.9 µM	K_d = 169.0 ± 4.3 µM	K_d = 7.9 ± 1.0 µM	K_d = 53.0 ± 0.4 µM
n ~ 0.9	n ~ 1	n ~ 0.9	n ~ 0.9
ΔH = -2287 ± 392 cal/mol	ΔH = -3984 ± 258 cal/mol	ΔH = -5590 ± 240 cal/mol	ΔH = -4809 ± 612 cal/mol

Fig. S1. Isothermal titration calorimetry studies of the binding of MetNIQ and MetQ variants to D-methionine and D-selenomethionine

ITC titrations of MetQ variants, including wildtype (wt) MetQ and N229A MetQ (NA MetQ) to D-methionine (A, B) and D-selenomethionine (D-semet) (C, D), respectively.

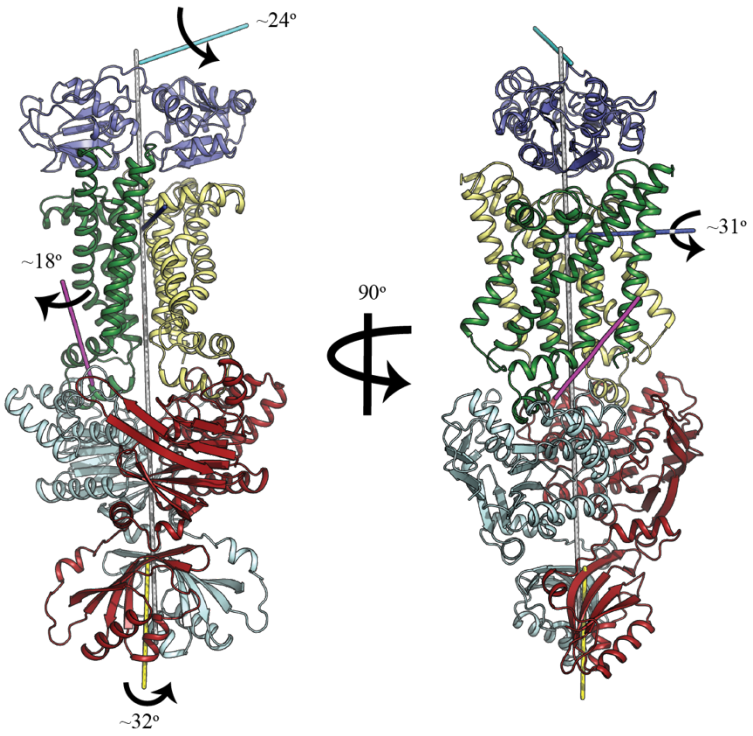

Fig. S2. Relationships between the inward and outward facing MetNIQ structures

Comparison of the relationships between subunits and domains of the OWF MetNIQ structure to those of the free methionine-bound (holo-) MetQ and IWF MetNI structures. The rotation axes (depicted as colored rods with corresponding rotation angles in degrees) were calculated from the transformations associated with superimposing the appropriate subunits or domains of the OWF (reported here) and IWF (PDB 3TUI) structures. The rotation axes are shown for the conversion between holo-MetQ and the structure in the MetNIQ complex (cyan), and for the interconversion between IWF and OWF conformations for the transmembrane MetI (red), the MetN nucleotide binding domains (magenta), and the C2 domains (blue).

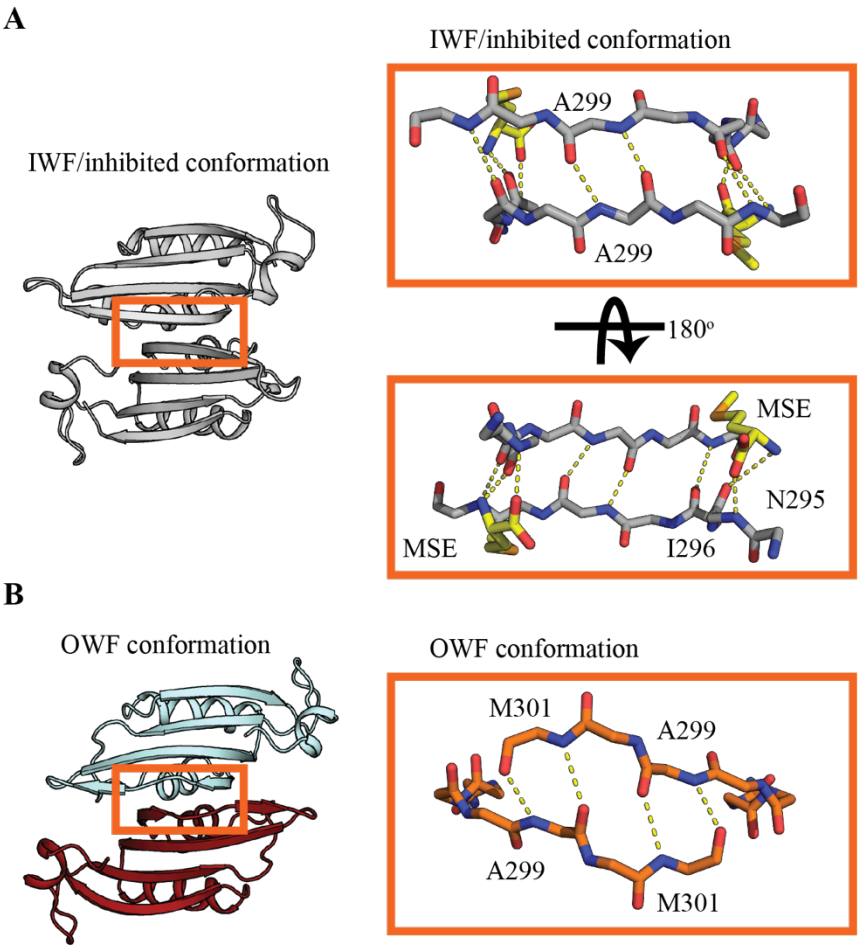

Fig. S3. Hydrogen-bonding shifts at the interface of C2 domains

View down the molecular twofold axis of the C2 domains illustrating the rearrangements associated with the transition between (A) the inward facing and (B) outward facing conformations. The panels on the right illustrate the accompanying shifts in hydrogen-bonding network (yellow dashes) in the β-sheet at the interface between C2 dimers. In the IWF conformation, residue A299 from one C2 domain forms interstrand hydrogen bonds to the same residue on the other domain, while in the OWF state, the A299 is hydrogen bonded to M301 from the other C2 domain. Binding of L-selenomethionine (MSE) helps stabilize the IWF conformation by interacting with N295 across the C2 domain dimer interface (PDB: 3TUZ).

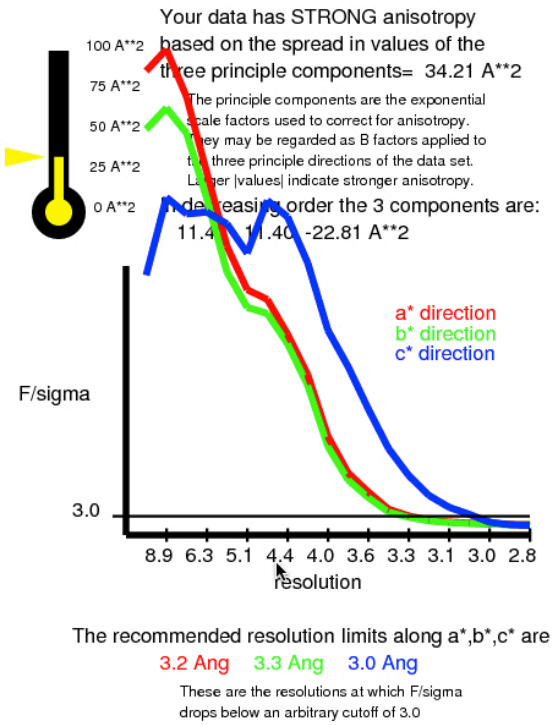

Fig. S4. Ellipsoidal truncation and anisotropic scaling of the MetNIQ diffraction data

Diffraction data collected from a MetNIQ crystal were ellipsoidally truncated and scaled by the UCLA MBI Diffraction Anisotropy Server (http://services.mbi.ucla.edu/anisoscale). Data were truncated along the directions a*, b*, and c* to resolution 3.2 Å, 3.3 Å and 3.0 Å respectively, where F/sigma drops below 3.0.

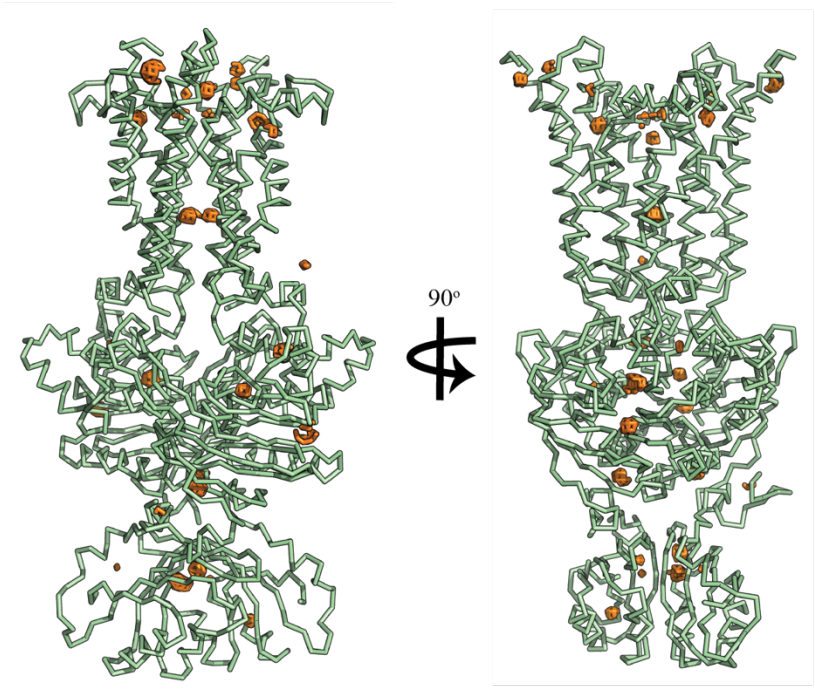

Fig. S5. Anomalous difference Fourier map

The anomalous difference Fourier map, contoured at 4.5 σ (standard deviation of the map; orange mesh) was calculated from the selenomethionine SAD data with heavy-atom (selenium) sites derived from MR-SAD experimental phasing. MetQ contains no methionines and is omitted in this figure.

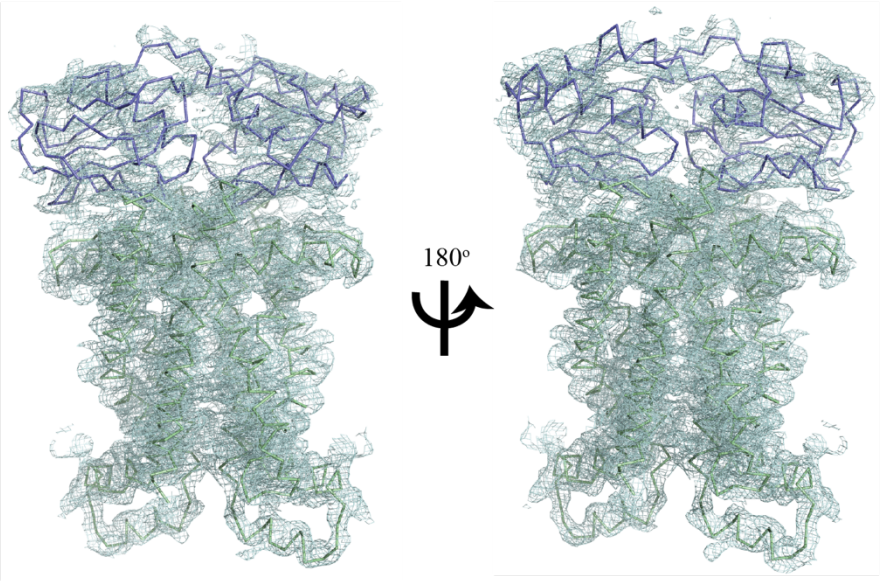

Fig. S6. Electron density map covering the MetQ and MetI subunits

The electron density map covering the MetQ and MetI subunits (pale cyan mesh), contoured at 1σ, with the Cα backbones depicted for MetQ (colored slate) and MetI (colored pale green). The map was calculated using the SIGMAA weighted amplitudes and phases following refinement of MetNIQ at 2.95 Å resolution.

Table S1. Data collection and refinement statistics for MetNIQ (after ellipsoidal truncation and anisotropic scaling)

Crystal	Hg-derivatized MetNIQ	Semet-substituted MetNIQ
Wavelength (Å)	1.006	0.9794
Resolution range (Å)	39.85 - 2.954 (3.06 - 2.954)	39.67 - 3.83 (4.13 – 3.83)
Space group	P 3_2 2 1	P3_2 2 1
Unit cell (a, c (Å))	107.96, 354.52	108.44, 349.12
Total reflections	820977 (9198)	232585 (46442)
Unique reflections	43069 (534)	23735 (4691)
Multiplicity	19.1 (17.0)	9.8 (9.9)
Completeness (%)	83.54 (10.50)	99.40 (97.60)
Mean I/sigma(I)	15.04 (1.48)	6.8 (1.9)
Wilson B-factor (Å^2)	92.7	121.09
R-merge	0.129 (1.89)	0.342 (2.618)
R-meas	0.133 (1.95)	0.380 (2.914)
R-pim	0.0306 (0.458)	0.165 (1.267)
CC1/2	0.999 (0.568)	0.993 (0.527)
CC*	1 (0.851)	
Reflections used in refinement	42966 (535)	
Reflections used for R-free	2173 (29)	
R-work	0.209 (0.444)	
R-free	0.228 (0.511)	
CC(work)	0.867 (0.495)	

CC(free)	0.799 (0.451)	
Number of non-hydrogen atoms	10359	
macromolecules	10292	
ligands	67	
Protein residues	1344	
RMS (bonds) (Å)	0.010	
RMS (angles) (˚)	1.11	
Ramachandran favored (%)	93.10	
Ramachandran allowed (%)	6.75	
Ramachandran outliers (%)	0.15	
Rotamer outliers (%)	2.04	
Clashscore	8.47	
Average B-factor ($Å^2$)	108.42	
macromolecules	108.64	
ligands	75.27	
Number of TLS groups	31	

Statistics for the highest-resolution shell are shown in parentheses.

The diffraction dataset used in the refinement was collected from a K_2HgI_4 soaked crystal.

The twin fractions determined by Xtriage (Phenix) of the Hg-derivatized and Semet-substituted crystals are 0.28 and 0.10, respectively.